Mar Biodiv (2018) 48:603–620
DOI 10.1007/s12526-017-0758-4

SENCKENBERG

ORIGINAL PAPER

Deep-sea amphipod genus *Eurythenes* from Japan, with a description of a new *Eurythenes* species from off Hokkaido (Crustacea: Amphipoda: Lysianassoidea)

Yukiko Narahara-Nakano[1] · **Takafumi Nakano**[1] · **Ko Tomikawa**[1]

Received: 10 May 2017 / Revised: 15 June 2017 / Accepted: 16 June 2017 / Published online: 11 July 2017

Abstract Two species of the giant deep-sea amphipod genus *Eurythenes* are reported from two bathyal habitats in Japanese waters based on a morphological examination and DNA analyses. The new species *E. aequilatus* collected off Hokkaido in the Sea of Okhotsk comprises a distinctive lineage within the known *Eurythenes* species and genetic groups. This finding sheds light onto the overlooked role of the marginal deep sea in the species diversification history of *Eurythenes*. *Eurythenes* specimens collected from the south off Okinawa Island in the Philippine Sea were identified as *E. magellanicus*, confirming the presence of a population in the western North Pacific. Past and present trans-oceanic dispersal of this species is briefly discussed based on the mitochondrial DNA sequences obtained from the Okinawa specimens of *E. magellanicus*.

Keywords Eurytheneidae · Molecular phylogeny · Cryptic species · Pacific Ocean · Long-distance dispersal

This article is registered in ZooBank under urn:lsid:zoobank.org:pub:780459CE-5D7B-4ADE-B146-E1BFA6468A79

Communicated by A. Brandt

Electronic supplementary material The online version of this article (doi:10.1007/s12526-017-0758-4) contains supplementary material, which is available to authorized users.

✉ Takafumi Nakano
tnakano@hiroshima-u.ac.jp

[1] Department of Science Education, Graduate School of Education, Hiroshima University, 1-1-1 Kagamiyama, Higashihiroshima 739-8524, Japan

Introduction

The genus *Eurythenes* S.I. Smith in Scudder, 1882 consists of deep-sea giant lysianassoidean amphipods with body lengths reaching 15 cm (Baldwin and Smith 1987), recorded from across the world's oceans, except the Mediterranean and Red seas (Stoddart and Lowry 2004; d'Udekem d'Acoz and Havermans 2015). *Eurythenes* amphipods generally occur in bathyal, abyssal, and hadal habitats, but have also been found on the ocean surface (Thurston et al. 2002; De Broyer et al. 2007). The generic name *Eurythenes* was proposed as a replacement name for *Eurytenes* Lilljeborg, 1865 by S.I. Smith in Scudder (1882); thus, its type species is *Lysianassa magellanica* H. Milne Edwards, 1848, which was originally designated as the *Eurytenes* type species by Lilljeborg (1865).

Until the revision by Stoddart and Lowry (2004), the genus had contained only three nominal species, namely *E. gryllus* (Lichtenstein in Mandt, 1822), *E. magellanicus*, and *E. obesus* (Chevreux, 1905), although *E. magellanicus* was considered by many to be a junior synonym of *E. gryllus*. While Stoddart and Lowry (2004) described the fourth *Eurythenes* nominal species *E. thurstoni* Stoddart & Lowry, 2004 in east Australian waters, they retained *E. magellanicus* as a dubious junior synonym for *E. gryllus*. It was not until the extensive molecular phylogenetic study by Havermans et al. (2013) and the systematic revision by d'Udekem d'Acoz and Havermans (2015) that the genus was expanded to include seven species. d'Udekem d'Acoz and Havermans (2015) referred to the cosmopolitan *E. gryllus* as the *gryllus* complex, and described three new species, namely *E. andhakarae* d'Udekem d'Acoz & Havermans, 2015, *E. maldoror* d'Udekem d'Acoz & Havermans, 2015, and *E. sigmiferus* d'Udekem d'Acoz & Havermans, 2015, which were discriminated from the *gryllus* complex.

Eurythenes amphipods identified generally as *E. gryllus* or *E. obesus* have been reported from the Pacific deep sea east of the Japanese Archipelago (Umezu 1982, 1984; Hasegawa et al. 1986). However, these previous records were based on the past classification of the *Eurythenes* species treating the *gryllus* complex species as a single cosmopolitan *E. gryllus*. We examined the morphological and molecular characteristics of *Eurythenes* specimens newly collected from two Japanese localities and revealed their taxonomic status based on the ongoing species concept within the genus *Eurythenes*. We herein describe a new *Eurythenes* species discriminated from the *gryllus* complex as the eighth nominal species in the genus and provide the first record of *E. magellanicus* from Japanese waters.

Materials and methods

Eurythenes specimens were collected from two localities in Japanese waters, i.e., the south off Okinawa Island, the Ryukyu Islands, and the west off Shiretoko Peninsula, Hokkaido (Fig. 1). In both localities, amphipods were collected using a baited trap.

Prior to dissecting the specimens, drawing of whole bodies of the specimens was conducted using a stereoscopic microscope with a drawing tube (Leica M125). Then, their appendages were dissected in 99% ethanol and mounted in glycerol on glass slides under the microscope. These slides were examined using a compound microscope (Olympus BH-2) and illustrated with the aid of a camera lucida. Specimens examined in this study have been deposited in the Zoological Collection of Kyoto University (KUZ). The setal and mouthpart terminology follows Lowry and Stoddart (1995).

Genomic DNA was extracted from muscle tissues following the method described by Nakano (2012a). Primer sets for the polymerase chain reaction (PCR) and cycle sequencing (CS) reactions used for 28S rRNA (28S), histone H3 (H3), and cytochrome *c* oxidase subunit I (COI) in this study are shown in Tomikawa et al. (2016a) and that for 16S rRNA (16S) is indicated in Havermans et al. (2013). The PCR reactions and DNA sequencing were performed using a modified version of a method reported in Nakano (2012b) and Tomikawa et al. (2016b), and detailed PCR conditions for 28S, H3, and COI were identical to those in Tomikawa et al. (2016a). The PCR reaction mixtures for 16S were heated to 94 °C for 6 min, followed by 35 cycles at 94 °C (10 s), 44 °C (20 s), and 72 °C (36 s), and a final extension at 72 °C for 6 min. In total, 12 sequences from the Japanese *Eurythenes* specimens were newly obtained in this study and deposited with the

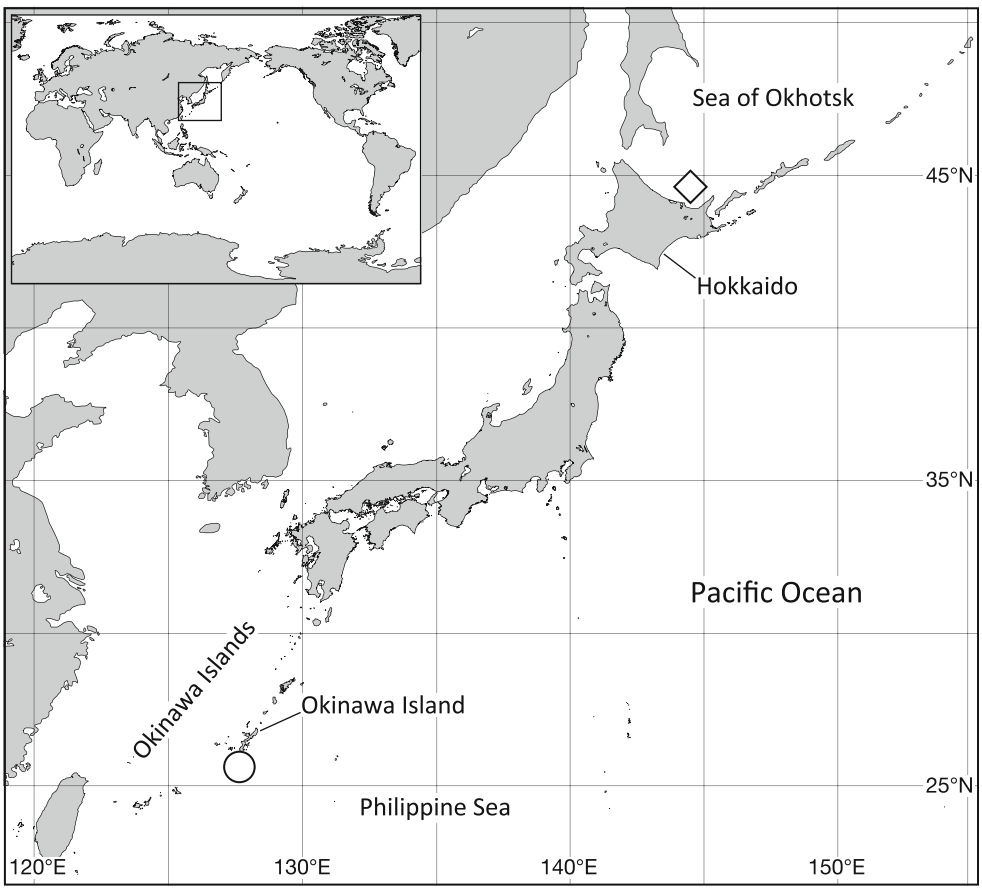

Fig. 1 Map showing the collection localities of the specimens examined in this study. The *white diamond* shows the locality of the *Eurythenes* species newly described in this study. The *white circle* denotes the locality of *E. magellanicus* specimens

International Nucleotide Sequence Database Collaboration (INSDC) through the DNA Data Bank of Japan.

To determine the phylogenetic positions of the present Japanese *Eurythenes* specimens, 161 sequences published in previous studies (France and Kocher 1996; Escobar-Briones et al. 2010; Havermans et al. 2013; Corrigan et al. 2014; Ritchie et al. 2015; Eustace et al. 2016; Havermans 2016) were obtained from the INSDC for use in molecular phylogenetic analyses (Table S1). Additionally, a COI sequence of *E. obesus* (Eob-C103) was obtained from d'Udekem d'Acoz and Havermans (2015) (Table S1). Two lysianassoidean species, *Bathycallisoma schellenbergi* (Birstein & Vinogradov, 1958) and *Paracallisoma* sp., were used as outgroup taxa.

Phylogenetic trees were reconstructed using 28S, COI, and 16S markers: those were estimated based on respective markers, as well as concatenated sequences of these three markers. The alignment of COI was trivial, as no indels were observed. The 28S and 16S sequences were aligned using MAFFT v7.310 L-INS-i (Katoh and Standley 2013). When completely identical sequence pairs were detected in the datasets, then one of each pair was removed using the "pgelimdupseq" command implemented in Phylogears v2.0.2014.03.08 (Tanabe 2008).

Phylogenetic relationships were estimated using maximum likelihood (ML) and Bayesian inference (BI). ML phylogenies were conducted using RAxML v8.2.8 (Stamatakis 2014), immediately after nonparametric bootstrapping (BS) with 1000 replicates. The best-fit models for each partition were identified with the Akaike information criterion using PartitionFinder v2.1.1 (Lanfear et al. 2017) with the "all" algorithm. BI and Bayesian posterior probabilities (PPs) were estimated using MrBayes v3.2.6 (Ronquist et al. 2012). The best-fit models for each partition were selected with the Bayesian information criterion using PartitionFinder with the "all" algorithm. Two independent runs of four Markov chains were conducted for 5 million generations for respective markers and for 10 million generations for the concatenated dataset: the tree was sampled every 100 generations. The parameter estimates and convergence were checked using Tracer v1.6.0 (Rambaut and Drummond 2013).

Systematics

Suborder Gammaridea Latreille, 1802
Superfamily Lysianassoidea Dana, 1849
Family Eurytheneidae Stoddart & Lowry, 2004
Genus *Eurythenes* Smith in Scudder, 1882
Eurythenes aequilatus sp. nov.
[New Japanese name: Hirome-okisokoebi]
(Figs. 2–8)

Material examined *Holotype.* KUZ Z1871, one female (105.4 mm), collected from Sea of Okhotsk, west off Shiretoko Peninsula, Hokkaido, Japan (St. 3 of R/V *Soyo-Maru* cruise), 44°35.0′N, 144°42.6′E–44°35.4′N, 144°41.8′E, 1574–1582 m deep, on 3 August 2009, by K. Kakui. *Paratypes.* KUZ Z1872, one female (111.0 mm), KUZ Z1873, one female (106.0 mm), and KUZ Z1874, one female (78.5 mm). Data same as for the holotype.

Description *Female* [holotype (KUZ Z1871)]. Body (Figs. 2 and 3) smooth, without setae. Pleonite 3 (Fig. 3) with anterior concavity. Posteroventral corner of epimeral plate 1 bluntly angular, that of plate 2 with tooth, that of plate 3 rounded. Head (Fig. 3) deeper than long, lateral cephalic lobe small, antennal sinus rounded; each of eyes with constant width, its ventral corner subtriangular, not narrowing distally.

Antenna 1 (Fig. 4a) 0.1 times as long as body length; accessory flagellum 11-articulate; primary flagellum 29-articulate; callynophore well-developed; calceoli absent.

Antenna 2 (Fig. 4b) 2.5 times as long as antenna 1, anterior margin of peduncular article 3–5 with brush setae; flagellum at least 72-articulate; calceoli absent.

Mouthpart bundle subquadrate. Epistome and upper lip (Fig. 4c) separate, epistome produced, angular; upper lip not produced, slightly rounded. Lower lip (Fig. 4d) with broad outer lobe, furnished with fine setae, inner lobe indistinct, mandibular lobe rounded. Mandibles (Fig. 4e–h) with right incisor weakly 2-dentate; left lacinia mobilis simple, vestigial; right lacinia mobilis absent; accessory setal row present; molar setose, not triturative; palp attached midway, 3-articulate. Maxilla 1 (Fig. 4i–k) inner plate with 8 plumose setae apically; outer plate with 12 spine-teeth in 9/3 crown arrangement; palp longer than outer plate, 2-articulate. Maxilla 2 (Fig. 4l) with inner plate broad and shorter than outer plate, both setose. Maxilliped (Fig. 5a, b) with inner plate subrectangular, bearing 3 nodular spines; outer plate subovate, with apical spines and plumose setae; palp 4-articulate, dactylus with unguis.

Gnathopod 1 (Fig. 5c, d) parachelate; coxa subquadrate, anteroventral corner and anteroventral margin with minute setae; basis broad, length 2.1 times width; posterodistal

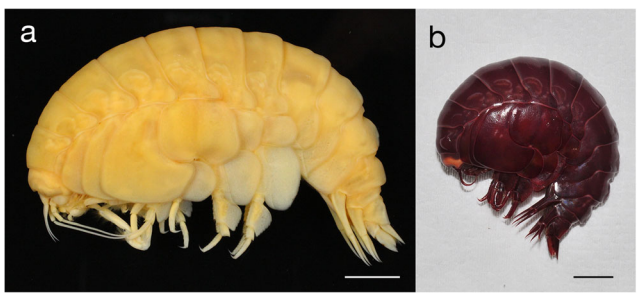

Fig. 2 *Eurythenes aequilatus* sp. nov., habitus, lateral views. **a** Female holotype (KUZ Z1871), 105.4 mm, in preservative. **b** An individual before fixation (photograph taken by K. Kakui). Scale bars: 10 mm

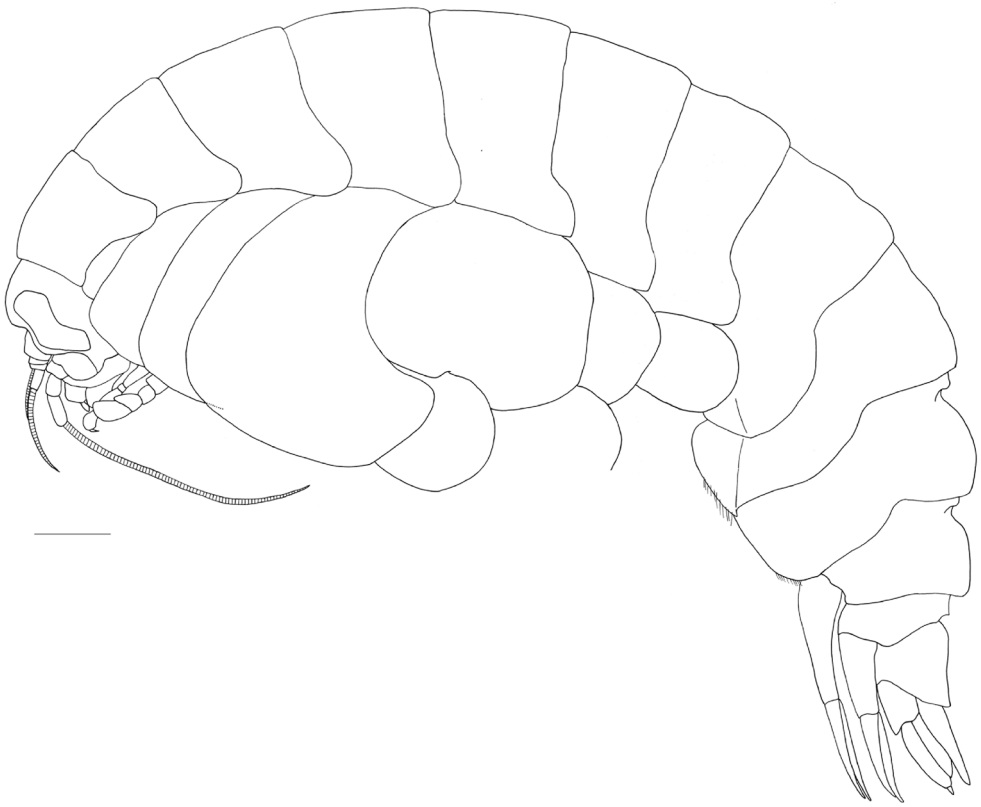

Fig. 3 *Eurythenes aequilatus* sp. nov., female holotype (KUZ Z1871), 105.4 mm. Habitus, lateral view, basis to dactylus of each of gnathopods 1 and 2 plus pereopods 3–7, and pleopods 1–3 omitted. Scale bar: 5 mm

corner of propodus with two robust setae, palm short, not produced, not exceeding 1/2 of posterior margin of dactylus.

Gnathopod 2 (Fig. 5e, f) minutely subchelate; coxa subrectangular, weakly curved ventrally, shorter than coxa 3; basis elongate, length 7.3 times width; posterior margin of merus rounded; propodus subrectangular, long, length 3.6 times width, palm slightly obtuse, with 3 medial robust setae; dactylus reaching palmar corner.

Pereopod 3 (Fig. 5g) coxa subrectangular; basis expanded posteriorly; merus expanded anteriorly; carpus stout; propodus and dactylus missing.

Pereopod 4 (Fig. 6a) subequal in size to pereopod 3, with well-developed posteroventral lobe of coxa, length 1.1 times width; merus expanded anteriorly; dactylus short, slender.

Pereopod 5 (Fig. 6b) coxa subquadrate, anterior and posterior lobes subequal; basis expanded posteriorly, posterior margin minutely crenate; merus expanded posteriorly, with curved posterior margin, its posterodistal lobe distally blunt; propodus with 6 groups of robust setae along anterior margin and 1 anterodistal robust seta; dactylus short, slender.

Pereopod 6 (Fig. 6c, d) coxa small, quadrate, not lobate posteriorly; basis expanded posteriorly, posterior margin minutely crenate; merus expanded posteriorly, with curved posterior margin, its posterodistal lobe distally blunt; propodus with 9 groups of robust setae along anterior margin and 1 anterodistal robust seta; dactylus short, slender.

Pereopod 7 (Fig. 6e) coxa subrectangular; basis expanded posteriorly, anterior length 1.1 times width, posterior margin minutely crenate; merus expanded posteriorly with curved posterior margin, its posterodistal lobe distally slightly acute; propodus with 9 groups of robust setae along anterior margin and 1 anterodistal robust seta; dactylus short, slender.

Coxal gills (Figs. 5e, g and 6a–c, e) on gnathopod 2 and pereopods 3–7. Oostegites (Figs. 5e, g and 6a, b) on gnathopod 2 and pereopods 3–5.

Pleopods (Fig. 7a–i) with 7 to 9 retinacula (Fig. 7b, e, h) and associated setae on inner distal corner of peduncle; medial margin of inner ramus with 4–18 bifid plumose setae (Fig. 7c, f, i).

Uropod 1 (Fig. 7j) peduncle bearing at least 50 dorsolateral, 2 apicolateral, 23 dorsomedial, and 1 apicomedial robust setae; outer ramus 0.8 times peduncle, bearing 22 lateral and 4 medial marginal robust setae; inner ramus 1.0 times outer ramus, bearing 7 lateral and 9 medial marginal robust setae. Uropod 2 (Fig. 7k) peduncle bearing 22 dorsolateral and 3 apicomedial,

Fig. 4 *Eurythenes aequilatus* sp. nov., female holotype (KUZ Z1871), 105.4 mm. **a** Right antenna 1, medial view. **b** Right antenna 2, medial view. **c** Upper lip, anterior view. **d** Lower lip, ventral view. **e** Left mandible, medial view. **f** Lacinia mobilis and accessory setal row of left mandible, medial view. **g** Right mandible, medial view. **h** Accessory setal row of right mandible, medial view. **i** Maxilla 1, dorsal view. **j** Outer plate of maxilla 1, dorsal view. **k** Distal part of palp article 2 of maxilla 1, dorsal view. **l** Maxilla 2, dorsal view. Scale bars: **a**–**e**, **g**, **i**, **l** = 1 mm; **f**, **h**, **k** = 0.2 mm; **j** = 0.5 mm ▶

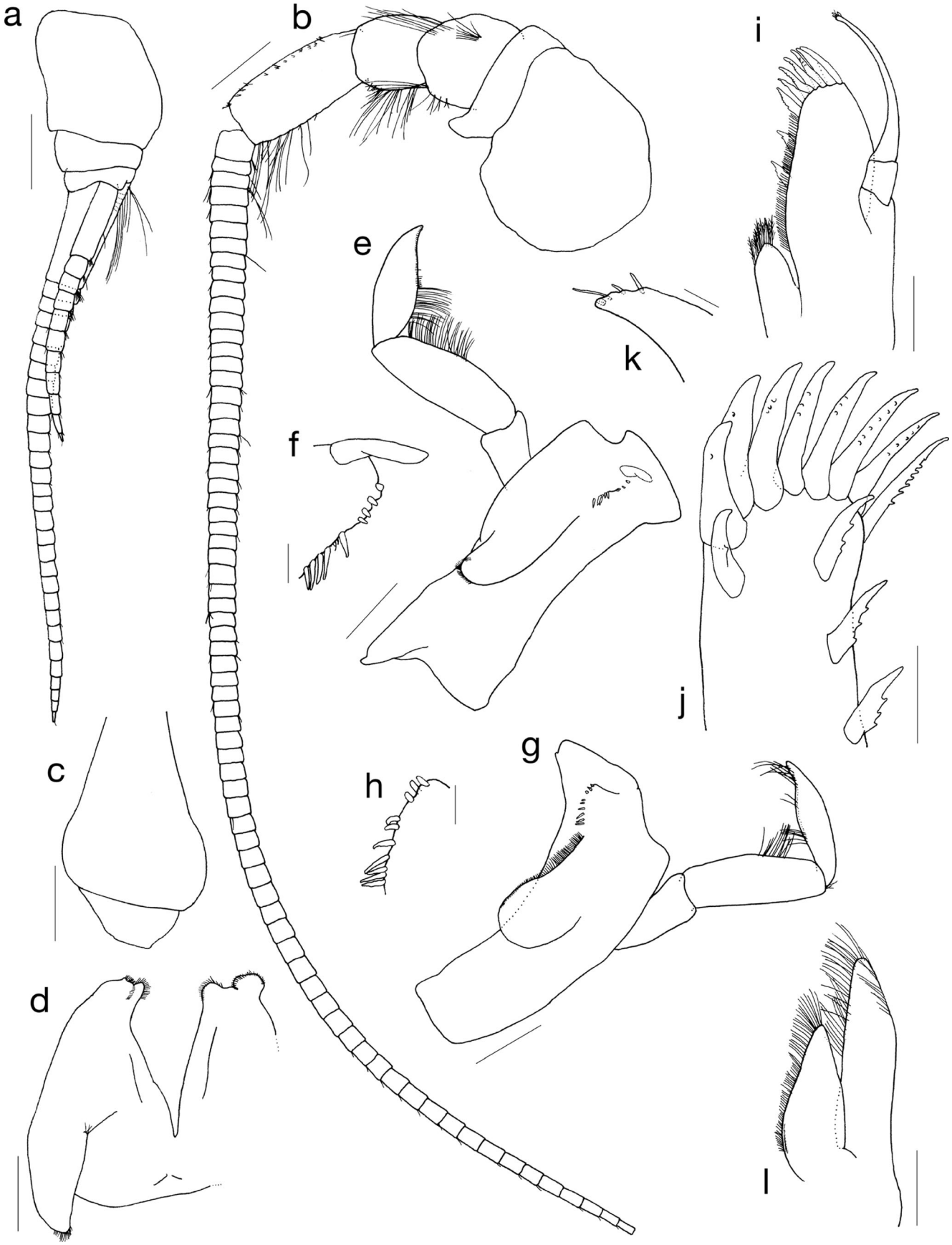
a
b
i
e
k
f
j
c
h
g
d
l

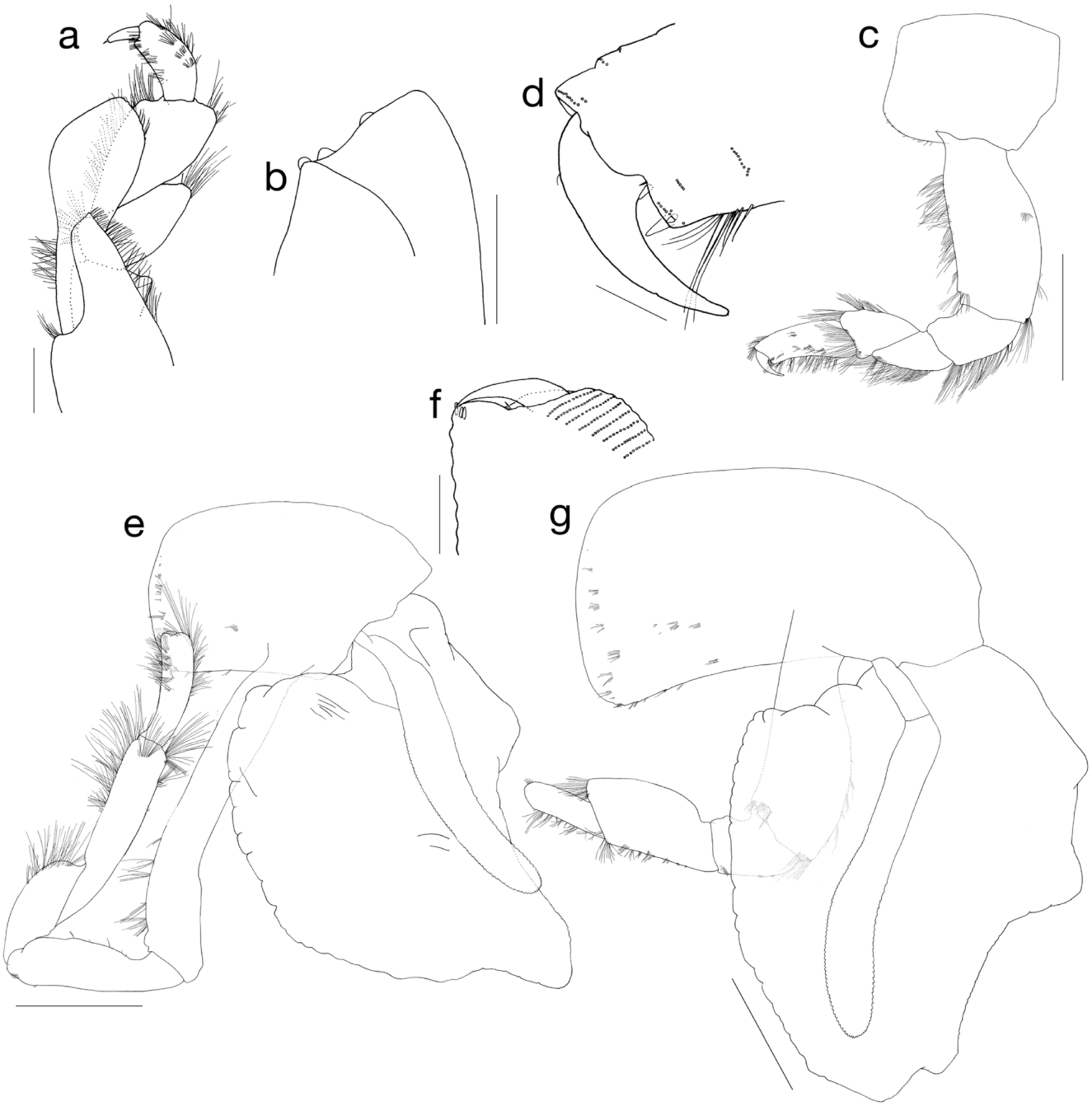

Fig. 5 *Eurythenes aequilatus* sp. nov., female holotype (KUZ Z1871), 105.4 mm. **a** Maxilliped (inner plate twisted outward), dorsal view. **b** Inner plate of maxilliped, dorsal view. **c** Right gnathopod 1, medial view. **d** Palmar margin of propodus and dactylus of right gnathopod 1, medial view. **e** Right gnathopod 2, with its oostegite and coxal gill 2, medial view. **f** Palmar margin of propodus and dactylus of right gnathopod 2, medial view. **g** Coxa to carpus of right pereopod 3, with its oostegite and coxal gill 3, medial view. Scale bars: **a** = 1 mm; **b**, **d**, **f** = 0.5 mm; **c**, **e**, **g** = 5 mm

16 dorsomedial robust setae; outer ramus 0.9 times peduncle, bearing 22 lateral and at least 5 medial marginal robust setae; inner ramus 1.1 times outer ramus, bearing 6 lateral and 9 medial marginal robust setae. Uropod 3 (Fig. 7l) laterodistal and mediodistal corners of peduncle with robust setae; outer ramus 2-articulate, medial margin of proximal article with

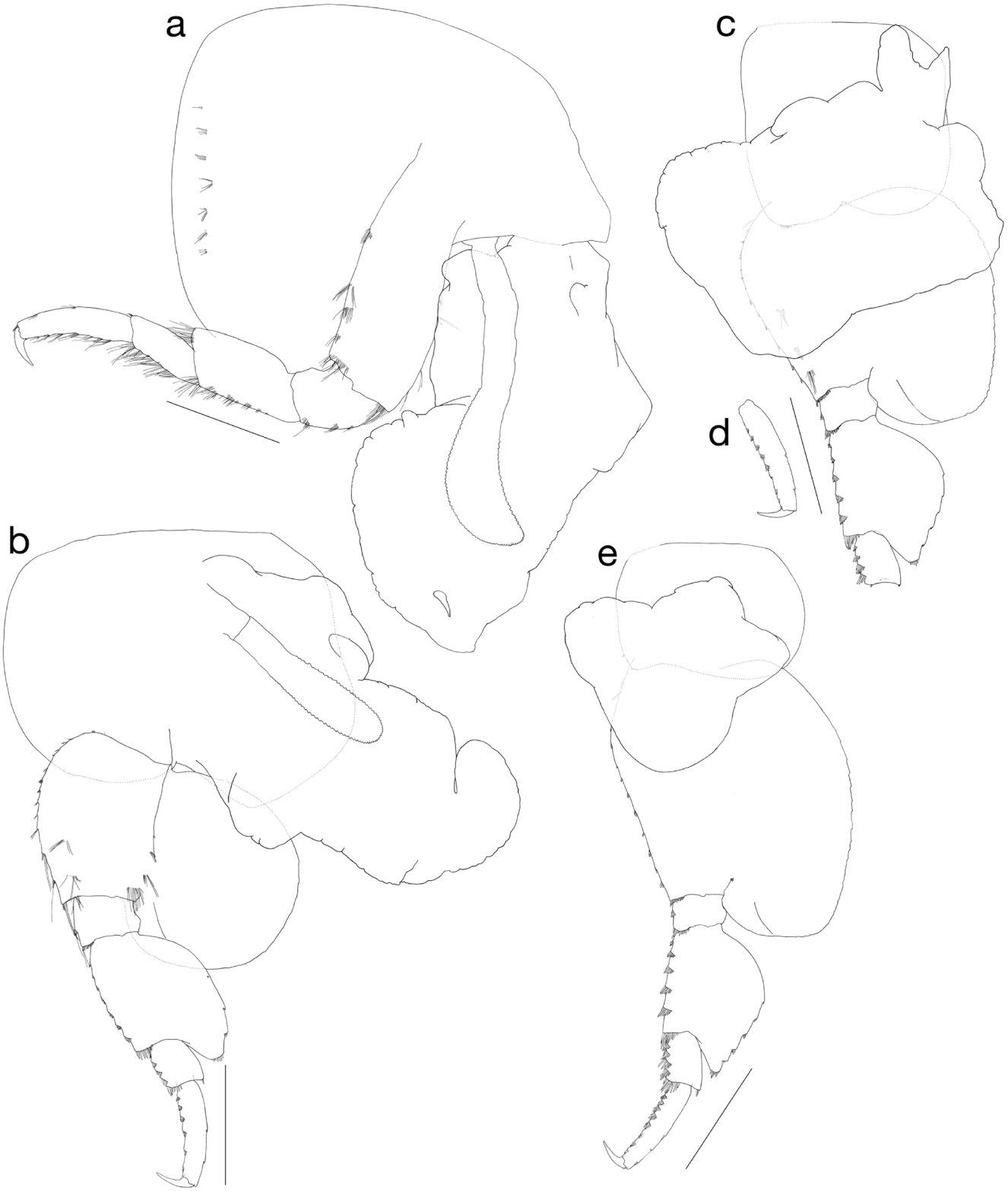

Fig. 6 *Eurythenes aequilatus* sp. nov., female holotype (KUZ Z1871), 105.4 mm. **a** Right pereopod 4, with its oostegite and coxal gill 4, medial view. **b** Right pereopod 5, with its oostegite and coxal gill 5, medial view. **c** Coxa to carpus of right pereopod 6, with coxal gill 6, medial view. **d** Propodus and dactylus of right pereopod 6, medial view. **e** Right pereopod 7, with coxal gill 7, medial view. Scale bars: 5 mm

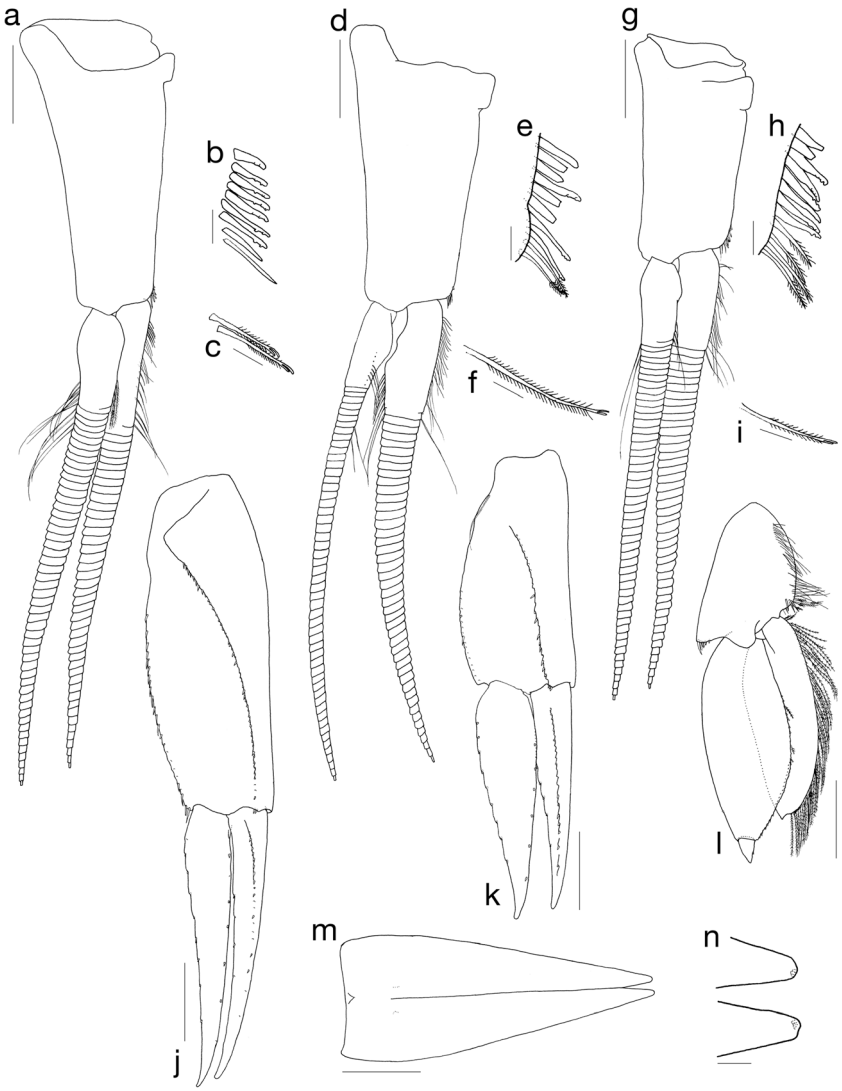

Fig. 7 *Eurythenes aequilatus* sp. nov., female holotype (KUZ Z1871), 105.4 mm. **a** Right pleopod 1, anterior view. **b** Retinacula on peduncle of right pleopod 1, anterior view. **c** Bifid plumose seta on inner medial margin of inner ramus of right pleopod 1, anterior view. **d** Right pleopod 2, anterior view. **e** Retinacula on peduncle of right pleopod 2, anterior view. **f** Bifid plumose seta on inner medial margin of inner ramus of right pleopod 2, anterior view. **g** Right pleopod 3, anterior view. **h** Retinacula on peduncle of right pleopod 3, anterior view. **i** Bifid plumose seta on inner medial margin of inner ramus of right pleopod 3, anterior view. **j** Right uropod 1, dorsal view. **k** Right uropod 2, dorsal view. **l** Right uropod 3, dorsal view. **m** Telson, dorsal view. **n** Distal part of telson, dorsal view. Scale bars: **a**, **d**, **g**, **j**–**m** = 2 mm; **b**, **c**, **e**, **f**, **h**, **i**, **n** = 0.2 mm

plumose setae; inner ramus subequal in length to proximal article of outer ramus, medial margin with numerous plumose setae.

Telson (Fig. 7m, n) elongate, cleft for ~84% of length, dorsal surface without robust setae, distal margin not incised, without apical setae.

Variation Maxilla 1 outer plate with 11 spine-teeth in 8/3 crown arrangement (Fig. 8); uropod 1 peduncle bearing 21 (KUZ Z1874), 42 (KUZ Z1873), or 49 (KUZ Z1872) dorsolateral robust setae; telson cleft for 72–79% of length.

Coloration In life, body red-purple; eyes whitish amber (Fig. 2b). Color faded in preservative.

DNA sequences In total eight DNA sequences were determined: for holotype (KUZ Z1871), 28S (INSDC accession number, LC229092; 1291 bp), H3 (LC229096; 328 bp), COI (LC229094; 658 bp), and 16S (LC229090; 481 bp); and for paratype (KUZ Z1872), 28S (LC229093; 1291 bp),

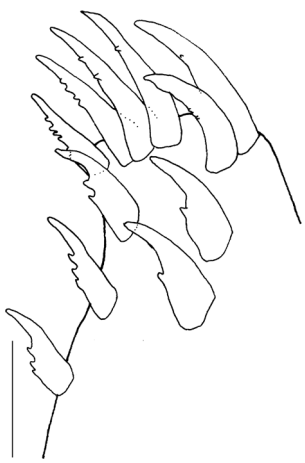

Fig. 8 *Eurythenes aequilatus* sp. nov., female paratype (KUZ Z1872), 111.0 mm. Outer plate of maxilla 1, dorsal view. Scale bar: 0.5 mm

Fig. 9 *Eurythenes magellanicus* (H. Milne Edwards, 1848), male (KUZ Z1875), 76.4 mm, from off Okinawa Island. Habitus, lateral view, in preservative. Scale bar: 5 mm

H3 (LC229097; 328 bp), COI (LC229095; 658 bp), and 16S (LC229091; 481 bp).

Etymology The specific name is a compound adjective derived from the Latin words *aequus* (equal) and *latus* (wide), referring to the fact that the eyes of this species are generally of constant width, a diagnostic character of the species.

Remarks *Eurythenes aequilatus* closely resembled *E. gryllus*, as judged by the following characteristics (Stoddart and Lowry 2004; d'Udekem d'Acoz and Havermans 2015): body smooth; pleonite 3 with anterior concavity; lateral cephalic lobe small; inner plate of maxilliped bearing 3 nodular spines; coxa of gnathopod 2 broad and weakly curved ventrally; palm of propodus of gnathopod 2 slightly obtuse; each of dactyli of pereopods 3–7 shorter than 0.6 each propodus. In particular, the characteristics of the head, and the number of nodular spines of the maxilliped inner plate are concordant with those of *E. gryllus*. Additionally, the number of groups of robust setae along the anterior margins of propodi of pereopods 5–7 of the Okhotsk specimens are identical to those of the holotype (Stoddart and Lowry 2004). Although the *E. aequilatus* holotype possesses a telson that is cleft >84% of its length (69% in the *E. gryllus* holotype), these values in the *E. aequilatus* paratypes overlap with those of other *E. gryllus* specimens (Stoddart and Lowry 2004; d'Udekem d'Acoz and Havermans 2015).

However, *E. aequilatus* can be distinguished from *E. gryllus* by the following characteristics [character states of *E. gryllus* defined by Stoddart and Lowry (2004) and d'Udekem d'Acoz and Havermans (2015) are in parentheses]: ventral corner of eye subtriangular, not narrowing distally (acute and narrowing distally); left lacinia mobilis simple, vestigial (distally slightly dentate); palm of propodus of gnathopod 1 not exceeding 1/2 of posterior margin of dactylus (exceeding); and posterodistal lobe of merus of pereopod 6 distally blunt (generally acute, but slightly blunt in holotype). Moreover, the results of the present molecular analyses showed that Okhotsk *Eurythenes* individuals formed a unique lineage among *Eurythenes* amphipods (see below). Based on the morphological and molecular distinctiveness of the Okhotsk specimens among known *Eurythenes* species, they are herein described as a new species named *E. aequilatus*.

Large specimens of *E. aequilatus* (body length >100 mm) possess 42–50 dorsolateral robust setae on uropod 1. As the small individual (KUZ Z1874; body length 78.5 mm) bears only ~20 setae on uropod 1, this character state may relate to the life stage of individuals of this species. However, it is

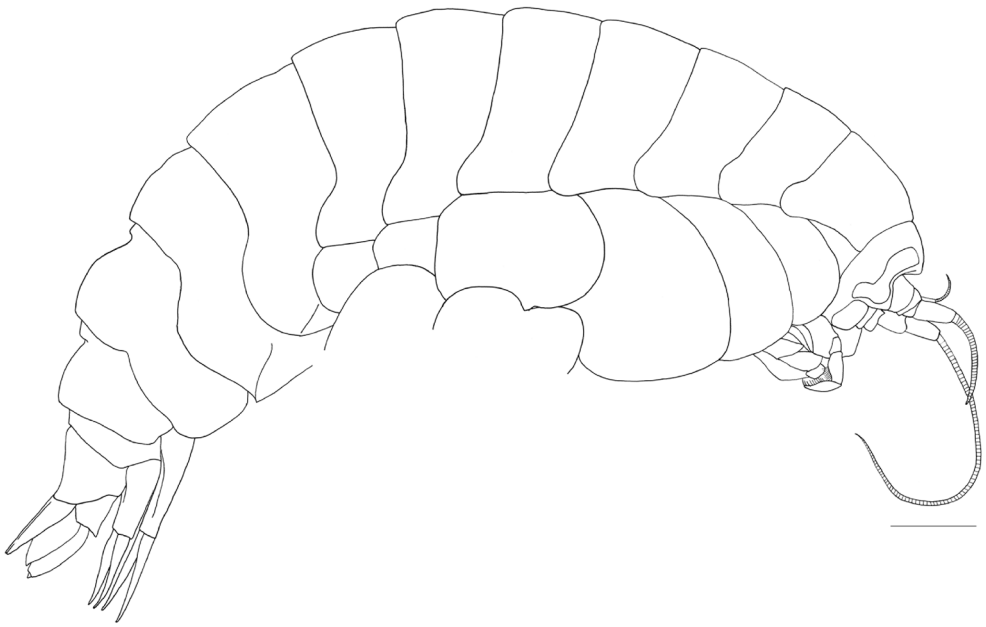

Fig. 10 *Eurythenes magellanicus* (H. Milne Edwards, 1848), male (KUZ Z1875), 76.4 mm, from off Okinawa Island. Habitus, lateral view, basis to dactylus of each of gnathopods 1 and 2 plus pereopods 3–7, and pleopods 1–3 omitted. Scale bar: 5 mm

possible that this characteristic distinguishes large individuals of *E. aequilatus* from equal-sized amphipods of the other *Eurythenes* species.

Eurythenes magellanicus (H. Milne Edwards, 1848)
[New Japanese name: Kobu-okisokoebi]
(Figs. 9–14)

Material examined KUZ Z1875, one male (76.4 mm), KUZ Z1876, one female (40.1 mm), and KUZ Z1877, four females (33.0–39.6 mm), collected from Philippine Sea, south off Okinawa Island, Ryukyu Islands, Japan, 25°49.605′N, 127°35.158′E, 1400 m, on 21 September 2012, by A. Kaneko and K. Yamada.

Description *Male* [KUZ Z1875]. Body (Figs. 9 and 10) smooth, without setae. Pleonite 3 (Fig. 10) with anterior concavity. Posteroventral corner of epimeral plate 1 weakly obtusely angular, that of plate 2 with tooth, that of plate 3 rounded. Head (Fig. 10) deeper than long, lateral cephalic lobe strongly produced, antennal sinus quadrate; each of eyes with inconstant width, its middle part narrowing, its ventral corner blunt and pointing obliquely backwards.

Antenna 1 (Fig. 11a, b) 0.1 times as long as body length; accessory flagellum 12-articulate; primary flagellum 33-articulate; callynophore well-developed; calceoli present (Fig. 11b).

Antenna 2 (Fig. 11c, d) 2.3 times as long as antenna 1, anterior margin of peduncular article 3–5 with brush setae; flagellum 81-articulate; calceoli present (Fig. 11d).

Mouthpart bundle subquadrate. Epistome and upper lip (Fig. 11e) separate, epistome produced, angular; upper lip not produced, slightly rounded. Lower lip (Fig. 11f) with broad outer lobe, furnished with fine setae, inner lobe indistinct, mandibular lobe rounded. Mandibles (Fig. 11g–j) with left and right incisors both 2-dentate; left lacinia mobilis vestigial, distally slightly dentate; right lacinia mobilis absent; accessory setal row present; molar setose, not triturative; palp attached midway, 3-articulate. Maxilla 1 (Fig. 11k, l) inner plate with 5 plumose setae apically; outer plate with 11 spine-teeth in an 8/3 crown arrangement; palp longer than outer plate, 2-articulate. Maxilla 2 (Fig. 11m) with inner plate slender and shorter than outer plate, both setose. Maxilliped (Fig. 12a, b) with inner plate subrectangular, bearing 4 nodular spines; outer plate subovate, with apical spines and plumose setae; palp 4-articulate, dactylus with unguis.

Gnathopod 1 (Fig. 12c, d) parachelate; coxa subquadrate, anteroventral margin and posteroventral corner with minute setae; basis broad, length 2.5 times width; posterodistal corner of propodus without robust setae, palm short, not produced.

Gnathopod 2 (Fig. 12e, f) minutely subchelate; coxa broad and weakly curved ventrally, shorter than coxa 3; basis elongate, length 5.7 times width; posterior margin of merus rounded; propodus subrectangular, long, length 3.2 times width, palm slightly obtuse, with 4 medial robust setae; dactylus not reaching palmar corner.

Fig. 11 *Eurythenes magellanicus* (H. Milne Edwards, 1848), male (KUZ Z1875), 76.4 mm, from off Okinawa Island. **a** Left antenna 1, medial view. **b** Article of left antenna 1 with calceolus, medial view. **c** Left antenna 2, medial view. **d** Articles of left antenna 2 with calceoli, medial view. **e** Upper lip, anterior view. **f** Lower lip, ventral view. **g** Left mandible, medial view. **h** Lacinia mobilis and accessory setal row of left mandible, medial view. **i** Right mandible, medial view. **j** Accessory setal row of right mandible, medial view. **k** Maxilla 1, dorsal view. **l** Outer plate of maxilla 1, dorsal view. **m** Maxilla 2, dorsal view. Scale bars: **a**, **c**, **e**–**g**, **i**, **k**, **m** = 1 mm; **b**, **d** = 0.1 mm; **h**, **j** = 0.2 mm; **l** = 0.5 mm

Pereopod 3 (Fig. 12g) coxa subrectangular; basis expanded posteriorly; merus expanded anteriorly; propodus stout; dactylus short, slender.

Pereopod 4 (Fig. 13a) subequal in size to pereopod 3, with well-developed posteroventral lobe of coxa, length 1.1 times width; merus expanded anteriorly; dactylus short, slender.

Pereopod 5 (Fig. 13b) coxa subquadrate, anterior and posterior lobes subequal; basis expanded posteriorly, posterior margin minutely crenate; merus expanded posteriorly, with curved posterior margin, its posterodistal lobe distally rounded; propodus with 9 groups of robust setae along anterior margin and 1 anterodistal robust seta; dactylus short, slender.

Pereopod 6 (Fig. 13c) coxa small, quadrate, not lobate posteriorly; basis expanded posteriorly, posterior margin minutely crenate; merus expanded posteriorly, with curved posterior margin, its posterodistal lobe distally acute; propodus with 10 groups of robust setae along anterior margin and 1 anterodistal robust seta; dactylus short, slender.

Pereopod 7 (Fig. 13d) coxa subrectangular; basis expanded posteriorly, anterior length 1.1 times width, posterior margin minutely crenate; merus expanded posteriorly with curved posterior margin, its posterodistal lobe distally blunt; propodus with 10 groups of robust setae along anterior margin and 1 anterodistal robust seta; dactylus short, slender.

Coxal gills (Figs. 12e, g and 13) on gnathopod 2 and pereopods 3–7.

Pleopods (Fig. 14a–f) with 5 to 9 retinacula (Fig. 14b, d, f) and associated setae on inner distal corner of peduncle; medial margin of inner ramus with 6–17 bifid plumose setae.

Uropod 1 (Fig. 14g) peduncle bearing at least 34 dorsolateral, 20 dorsomedial, and 1 apicomedial robust setae; outer ramus 0.8 times peduncle, bearing 17 lateral and 7 medial marginal robust setae; inner ramus 1.0 times outer ramus, bearing 13 lateral and 10 medial marginal robust setae. Uropod 2 (Fig. 14h) peduncle bearing 21 dorsolateral and 1 apicomedial, 16 dorsomedial robust setae; outer ramus 0.9 times peduncle, bearing at least 10 lateral and 5 medial marginal robust setae; inner ramus 1.0 times outer ramus, bearing 10 lateral and 13 medial marginal robust setae. Uropod 3 (Fig. 14i) laterodistal and mediodistal corners of peduncle with robust setae; outer ramus 2-articulate, medial margin of proximal article with plumose

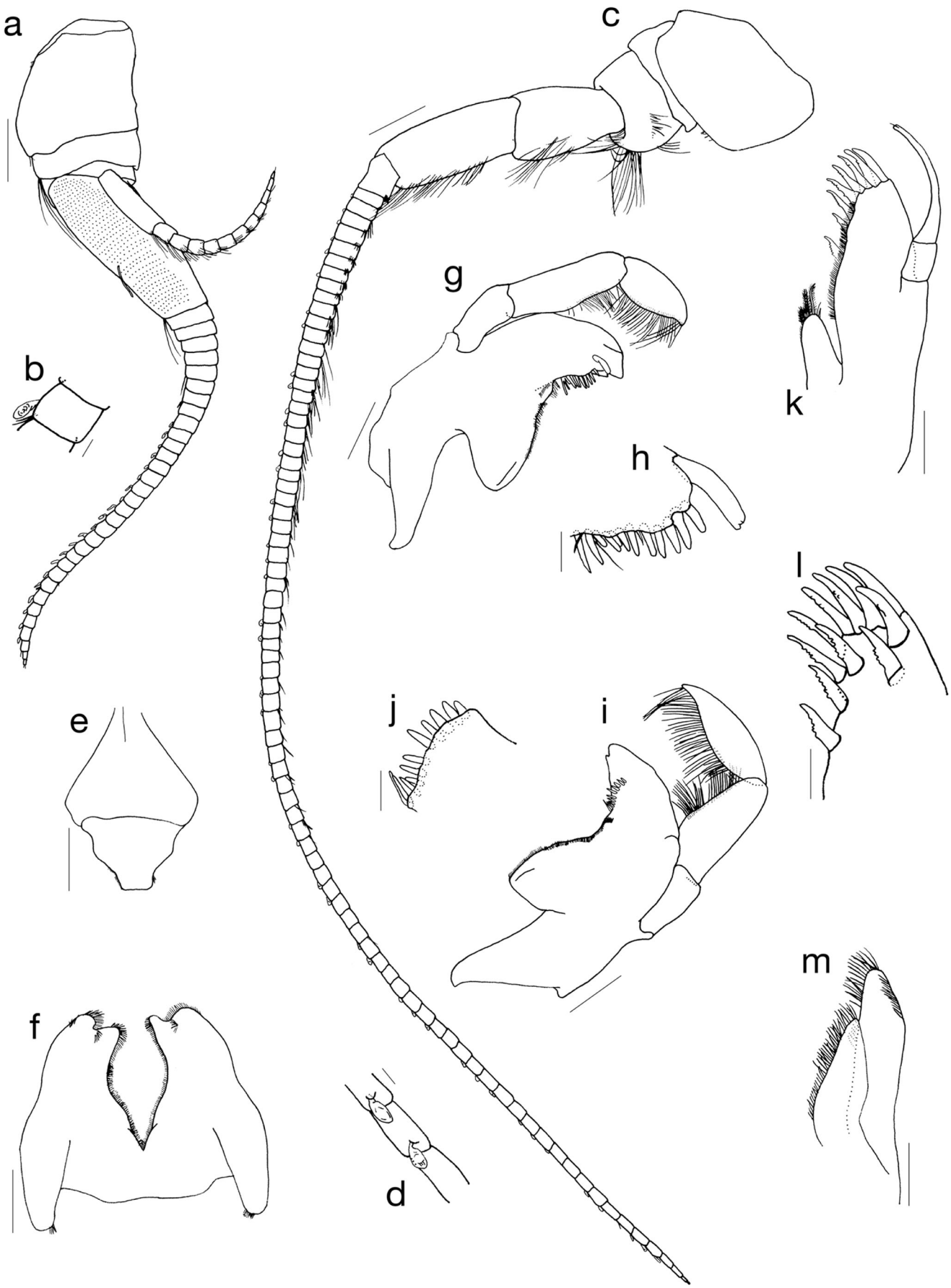
a
b
c
d
e
f
g
h
i
j
k
l
m

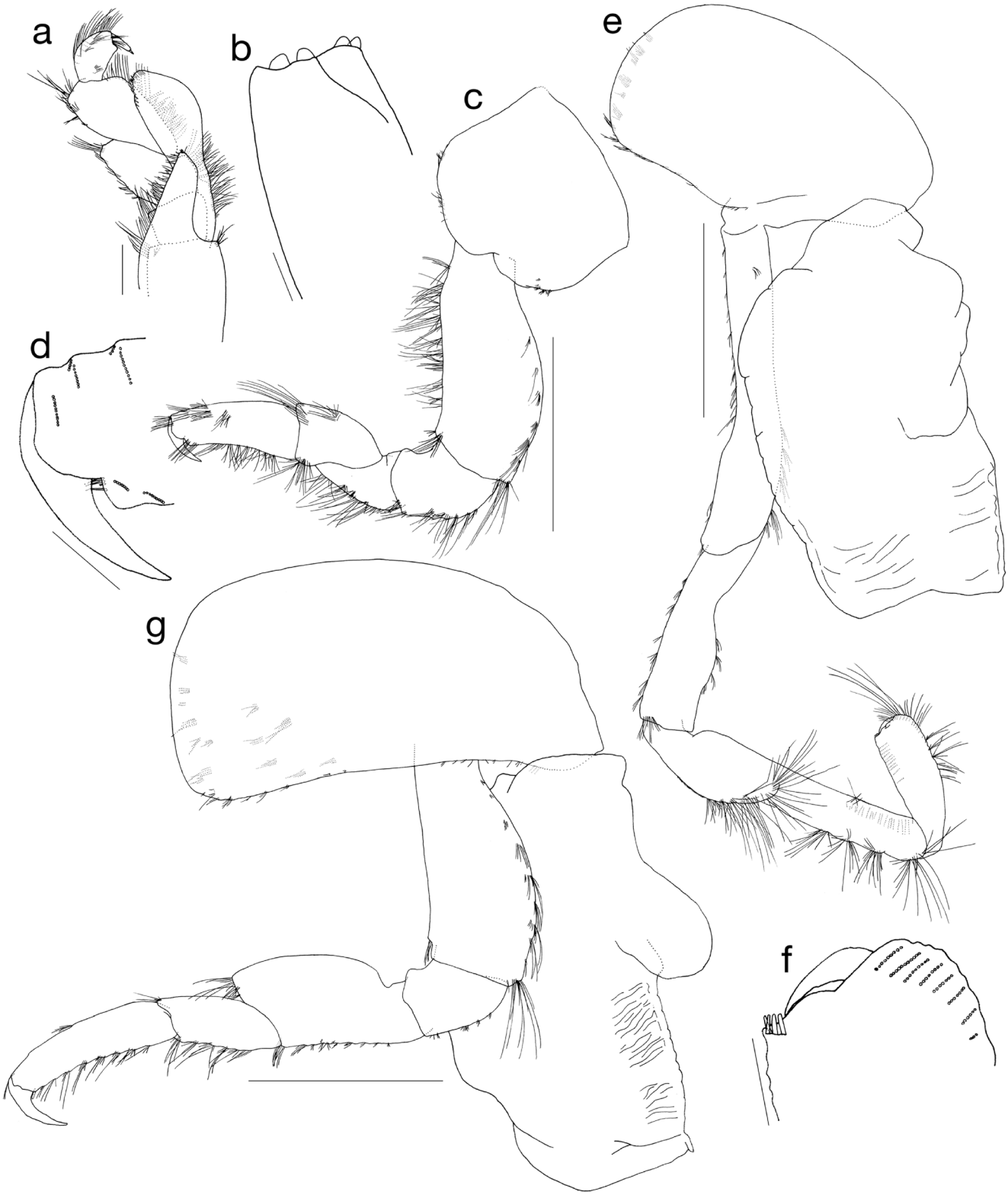

Fig. 12 *Eurythenes magellanicus* (H. Milne Edwards, 1848), male (KUZ Z1875), 76.4 mm, from off Okinawa Island. **a** Maxilliped (inner plate twisted outward), dorsal view. **b** Inner plate of maxilliped, dorsal view. **c** Left gnathopod 1, lateral view. **d** Palmar margin of propodus and dactylus of left gnathopod 1, lateral view. **e** Left gnathopod 2, with coxal gill 2, lateral view. **f** Palmar margin of propodus and dactylus of left gnathopod 2, lateral view. **g** Left pereopod 3, with coxal gill 3, lateral view. Scale bars: **a** = 1 mm; **b** = 0.2 mm; **c**, **e**, **g** = 5 mm; **d**, **f** = 0.5 mm

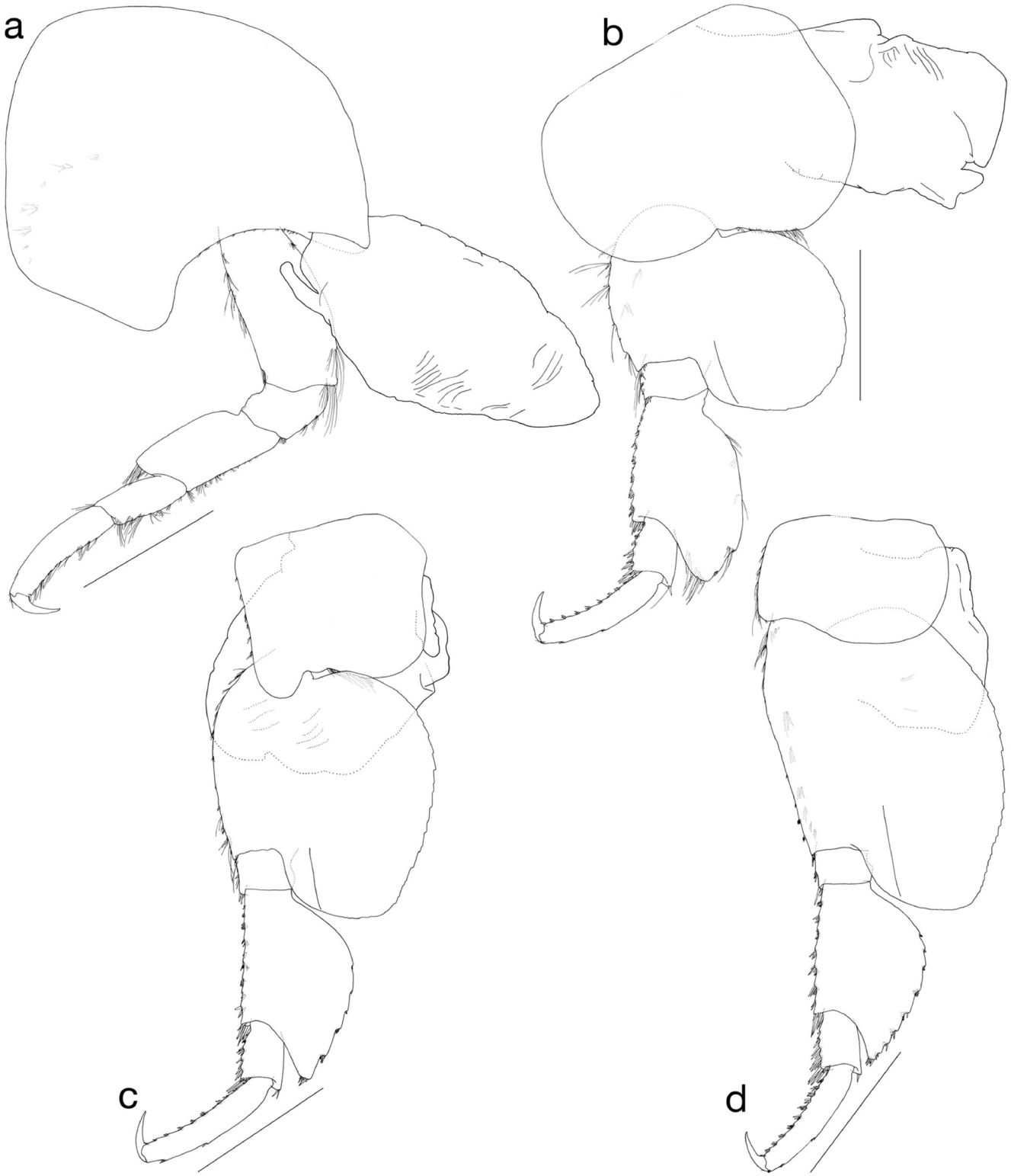

Fig. 13 *Eurythenes magellanicus* (H. Milne Edwards, 1848), male (KUZ Z1875), 76.4 mm, from off Okinawa Island. **a** Left pereopod 4, with coxal gill 4, lateral view. **b** Left pereopod 5, with coxal gill 5, lateral view. **c** Left pereopod 6, with coxal gill 6, lateral view. **d** Left pereopod 7, with coxal gill 7, lateral view. Scale bars: 5 mm

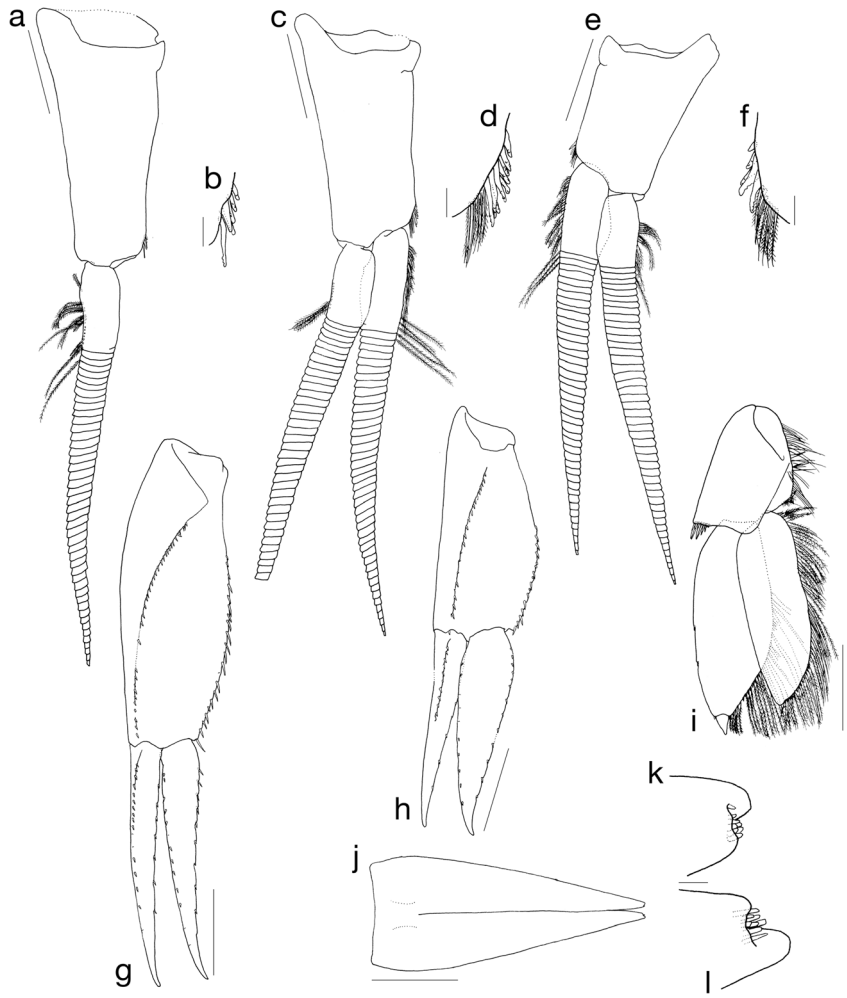

Fig. 14 *Eurythenes magellanicus* (H. Milne Edwards, 1848), male (KUZ Z1875), 76.4 mm, from off Okinawa Island. **a** Right pleopod 1, anterior view. **b** Retinacula on peduncle of right pleopod 1, anterior view. **c** Right pleopod 2, anterior view. **d** Retinacula on peduncle of right pleopod 2, anterior view. **e** Left pleopod 3, anterior view. **f** Retinacula on peduncle of left pleopod 3, anterior view. **g** Left uropod 1, dorsal view. **h** Left uropod 2, dorsal view. **i** Left uropod 3, dorsal view. **j** Telson, dorsal view. **k** Distal part of right lobe of telson, dorsal view. **l** Distal part of left lobe of telson, dorsal view. Scale bars: **a**, **c**, **e**, **g**–**j** = 2 mm; **b**, **d**, **f**, **k**, **l** = 0.2 mm

setae; inner ramus subequal in length to proximal article of outer ramus, medial margin with numerous plumose setae.

Telson (Fig. 14j–l) elongate, cleft for ~83% of length, dorsal surface without robust setae, distal margin incised, with 8 robust setae on each lobe.

Coloration Color in life unknown; faded in preservative.

DNA sequences Four nucleotide sequences of the examined specimen (KUZ Z1875) were determined: 28S (INSDC accession number, LC192880; 1291 bp), H3 (LC192882; 328 bp), COI (LC192881; 658 bp), and 16S (LC192879; 481 bp).

Remarks The Okinawa specimens were identified as *E. magellanicus* based on the presence of the following characteristics diagnosed by d'Udekem d'Acoz and Havermans (2015): body smooth; pleonite 3 with anterior concavity; lateral cephalic lobe strongly produced; eye with inconstant width, its ventral corner blunt and pointing obliquely backwards; inner plate of maxilliped bearing 4 nodular spines; coxa of gnathopod 2 broad and weakly curved ventrally; palm of propodus of gnathopod 2 obtuse; each of dactyli of pereopods 3–7 shorter than 0.6 each propodus. Additionally, the present specimens possessed 2-dentate incisors in the mandibles, a distally slightly dentate lacinia mobilis of the left mandible, and a telson cleft for ~80% of its length. These characteristics are concordant with those of the holotype and recently collected *E. magellanicus* specimens (Stoddart and Lowry 2004; d'Udekem d'Acoz and Havermans 2015).

The respective numbers of the groups of robust setae along the anterior margins of propodi of pereopods 5–7 and the anterodistal robust seta(e) are different from the known characteristics of *E. magellanicus* (previously recorded numbers in parentheses): propodus of pereopod 5, with 9 groups of robust setae along anterior margin and 1 anterodistal robust seta [9 groups and 2 anterodistal in Stoddart and Lowry (2004), and 8 groups in d'Udekem d'Acoz and Havermans (2015)]; of pereopod 6, 10 groups and 1 anterodistal [8 groups and 2 anterodistal in Stoddart and Lowry (2004), and 7 groups in d'Udekem d'Acoz and Havermans (2015)]; and of pereopod 7, 10 groups and 1 anterodistal [9 groups and 2 anterodistal in Stoddart and Lowry (2004), and 7 groups in d'Udekem d'Acoz and Havermans (2015)]. However, the molecular data clearly show that the present specimens belong to

E. magellanicus (see below); thus, those setal characteristics could be regarded as intraspecific morphological variations within the species.

Molecular analyses result

The phylogenetic analyses based on 28S sequences (1231 bp of alignment positions) were conducted using ten unique sequences including outgroup taxon. The two obtained 28S sequences from *E. aequilatus* were completely identical to each other. The best-fit model for the ML analysis was chosen as GTR + G; that for the BI analyses was identified as K80. Based on the results of the parameter estimates and convergence, the first 20,001 trees were discarded in the BI analyses. Both the obtained ML tree (ln L = −1877.45) and BI tree (mean ln L = −1904.02; Fig. 15a) failed to reveal the detailed relationships of the *Eurythenes* species. Each of *E. aequilatus* and the Japanese *E. magellanicus* formed the unique lineage among the *gryllus* complex OTUs.

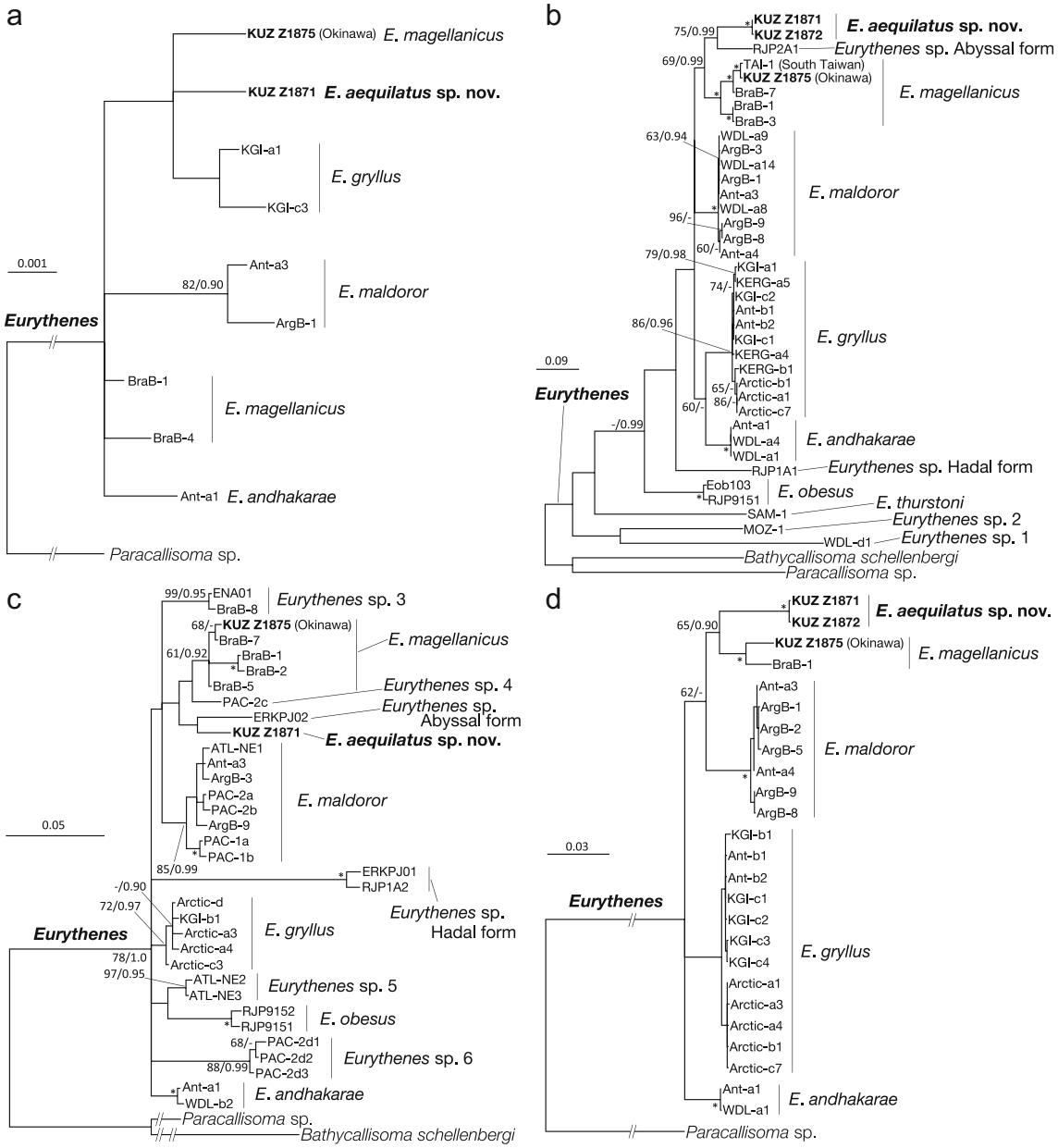

Fig. 15 Phylogenetic trees showing the phylogenetic positions of the present *Eurythenes* specimens. The numbers on nodes represent bootstrap values for maximum likelihood (BS; only values >49%) and Bayesian posterior probabilities (PPs; only values >0.89); the asterisks denote nodes with BS >89% and PPs >0.98. Sample numbers are shown in Table S1. **a** Bayesian inference tree for the 1231-bp nuclear 28S rRNA marker. **b** Maximum likelihood tree for the 658-bp mitochondrial cytochrome *c* oxidase I (COI) marker. **c** Bayesian inference tree for the 490-bp mitochondrial 16S rRNA marker. **d** Bayesian inference tree for the 2320-bp nuclear 28S and mitochondrial COI and 16S markers

The phylogenetic trees for 658 bp of COI was reconstructed based on 37 *Eurythenes* OTUs, along with two outgroup taxa. The best-fit model(s) and partition scheme for the ML analysis were chosen as GTR + I + G for every position of COI; those for the BI analyses were identified as SYM + I for the first position of COI, F81 + I for the second position of COI, and GTR + I + G for the third position of COI. The first 20,001 trees were discarded in the BI analyses. The obtained ML tree (ln L = −4220.89; Fig. 15b) had a topology almost identical to that of the BI tree (mean ln L = −3929.65; not shown). *Eurythenes aequilatus* formed a monophyletic lineage with *E. magellanicus* and the abyssal *Eurythenes* sp. defined by Ritchie et al. (2015) from the Peru–Chile Trench (BS = 69%, PP = 0.99). The monophyly of *E. aequilatus* and the abyssal *Eurythenes* sp. was also supported (BS = 75%, PP = 0.99). The specimen of *E. magellanicus* from off Okinawa (KUZ Z1875) was genetically close to the individual obtained from the southwest off Taiwan (TAI-1).

The 16S (490 bp alignment positions) phylogenetic analyses were performed based on the 34 *Eurythenes* OTUs with two outgroup taxa. Two 16S sequences of *E. aequilatus* were completely identical to each other; that obtained from the present *E. magellanicus* specimen (KUZ Z1875) and four sequences of the Peru–Chile Trench individuals (445 bp for RJP2B1 and RJP2B2, and 443 bp for ERKPJ05 and ERKPJ06, see Table S1) were completely identical to each other. Based on the result of the preliminary phylogenetic analyses, one sequence (ATL-NW3b) was removed from the dataset to prevent long branch attraction. The best-fit model for the ML analysis was chosen as GTR + I + G; that for the BI analyses was identified as HKY + G. The first 20,001 trees were discarded in the BI analyses. The obtained ML tree (ln L = −1915.45; not shown) had a topology almost identical to that of the BI tree (mean ln L = −1978.83; Fig. 15c). Although *E. aequilatus* formed a clade with the abyssal *Eurythenes* specimens (ERKPJ02 = ERKPJ03 = RJP2A1 = RJP2A2, see Table S1) obtained from the Peru–Chile Trench by Ritchie et al. (2015) and Eustace et al. (2016), this relationship was not supported in both ML and BI analyses. Moreover, *E. aequilatus* was highly diverged from the Peru–Chile Trench specimens. The present *E. magellanicus* specimen (KUZ Z1875) belonged to the monophyletic group consisting of *E. magellanicus* sequences (BS = 61%, PP = 0.92).

The phylogenetic trees for 2320 bp concatenated sequences of 28S (1178 bp), COI (658 bp), and 16S (484 bp) were constructed based on 25 *Eurythenes* OTUs and one outgroup taxon. The best-fit model(s) and partition scheme for the ML analysis were chosen as GTR + I + G for every position of COI, and respective 28S and 16S; those for the BI analyses were identified as K80 + I for each 28S and the first position of COI, F81 + I for the second position of COI, GTR + G for the third position of COI, and HKY + G for 16S. In the BI analyses, the first 40,001 trees were discarded. The obtained ML tree (ln L = −5346.35; not shown) had a topology almost identical to that of the BI tree (mean ln L = −5011.53; Fig. 15d). *Eurythenes aequilatus* and *E. magellanicus* formed a weakly supported clade in both analyses (BS = 65%, PP = 0.90). The monophyly of *E. aequilatus*, *E. magellanicus*, and *E. maldoror* was weakly supported in the obtained ML tree (BS = 62%).

Discussion

Eurythenes magellanicus has been recorded mainly from abyssal South American waters (~4500 m deep), i.e., Brazil Abyssal Basin, southwest Atlantic Ocean, and the Peru–Chile Trench, east Pacific Ocean (Havermans et al. 2013; Ritchie et al. 2015; Eustace et al. 2016); Havermans (2016) provided the first bathyal occurrence record of this species from the southwest off Taiwan (~1300 m), the South China Sea, western Pacific Ocean. Thus, the present study provides the second bathyal and western Pacific record of *E. magellanicus*, indicating that this species is indigenous to the bathyal habitats there.

The COI data show that the Okinawa and Taiwanese specimens of *E. magellanicus* are genetically very close to each other (Fig. 15b). Additionally, the Okinawa and Taiwanese individuals comprised a western Pacific clade within the abyssal Brazilian phylogroup of *E. magellanicus*. These results suggest that the common ancestor of the bathyal western Pacific *E. magellanicus* may have dispersed from the South Atlantic Ocean to the western Pacific via the Antarctic Circumpolar Current and the Circumpolar Deep Water in the Pacific Ocean (Kawabe and Fujio 2010). The Taiwanese population may have been introduced into the South China Sea from the Philippine Sea through the Luzon Strait, where the deep layer flows westward from the Philippine Sea (Zhang et al. 2015; Zhao et al. 2016), because this strait is the only deep connection (>2000 m) between the Pacific Ocean (= Philippine Sea) and the South China Sea, whereas the Okinawa population may have dispersed via the deep-water flow of the Ryukyu Current System along eastern Taiwan northeastward to the Okinawa Islands (Nagano et al. 2007; Thoppil et al. 2016).

The 16S data showed that the bathyal Okinawa *E. magellanicus* and abyssal Peru–Chile Trench individuals are closely related, sharing an identical sequence haplotype. Although the length of the analyzed sequences was quite short, this result suggests the possibility of gene flow between the bathyal northwestern Pacific and the abyssal southeastern Pacific populations. This close relationship between these two populations may also be maintained via the deep-water flow from the Philippine Sea east-southward to Central and South America (Kawabe and Fujio 2010). In any case, additional *E. magellanicus* samples from both regions and more

sensitive markers, e.g., microsatellites, are essential to elucidate the population genetic structure of Pacific *E. magellanicus*.

In contrast to *E. magellanicus* from Okinawa, *E. aequilatus* consisted of a unique lineage within the known *Eurythenes* species and genetic groups. Although the COI and 16S analyses showed the genetic relationships between *E. aequilatus* and the unidentified abyssal *Eurythenes* species from the Peru–Chile Trench, the DNA data revealed that these two species are highly diverged from each other, as in the intraspecific genetic divergences among the known *Eurythenes* species. The present *E. aequilatus* specimens were collected from the benthic habitat in the southernmost part of the Sea of Okhotsk, which comprises the deep Kuril Basin. This marginal sea connects to the western North Pacific through two deep straits (~2300 m) and additional shallow straits in the Kuril Islands (Talley 2001; Hill et al. 2003). The Sea of Okhotsk also connects to the Sea of Japan, but the strait between these two seas is quite shallow (~40 m). It has been suggested that the Okhotsk–Pacific water exchange, i.e., the outflow of the Sea of Okhotsk circulation, may be essentially small (Aramaki et al. 2001). It is highly possible that those features of the Sea of Okhotsk have harbored a unique lineage within *Eurythenes* as the distinctive species *E. aequilatus*.

The species diversity and evolutionary history of *Eurythenes* have been discussed based on specimens collected from bathyal to hadal habitats of the oceans (Havermans 2016). The present *E. aequilatus* findings highlight that marginal deep seas may also serve important roles in the diversification of this giant amphipod group. Further faunal surveys in marginal seas will be essential to depict the evolutionary history of *Eurythenes* species.

Acknowledgments The authors are grateful to Keiichi Kakui (Hokkaido University), Atsushi Kaneko (Okinawa Churaumi Aquarium, OCA), and Kenta Yamada (OCA) for providing valuable specimens of *Eurythenes* species. We also express our sincere thanks to Hidetoshi Nagamasu (The Kyoto University Museum) for his helpful advice on a specific name for the new species, and to Cédric d'Udekem d'Acoz (Royal Belgian Institute of Natural Sciences) and one anonymous reviewer for their constructive comments and suggestions on this manuscript. Thanks are extended to the captain and crew of the R/V *Soyo-Maru* (Japan Fisheries Research and Education Agency). This study was partly supported by JSPS KAKENHI grant numbers JP25242015, JP25840140, and JP15J00720.

References

Aramaki T, Watanabe S, Kuji T, Wakatsuchi M (2001) The Okhotsk-Pacific seawater exchange in the viewpoint of vertical profiles of radiocarbon around the Bussol' strait. Geophys Res Lett 28:3971–3974. doi:10.1029/2001GL013227

Baldwin RJ, Smith KL (1987) Temporal variation in the catch rate, length, color and sex of the necrophagous amphipod, *Eurythenes gryllus*, from the central and eastern North Pacific. Deep Sea Res Part I Oceanogr Res Pap 34:425–439. doi:10.1016/0198-0149(87)90146-4

Corrigan LJ, Horton T, Fotherby H, White TA, Hoelzel AR (2014) Adaptive evolution of deep-sea amphipods from the superfamily Lysiassanoidea in the North Atlantic. Evol Biol 41:154–165. doi:10.1007/s11692-013-9255-2

De Broyer C, Lowry JK, Jażdżewski K, Robert H (2007) Census of Antarctic marine life. Synopsis of the Amphipoda of the Southern Ocean. Edited by Calude de Broyer. Volume 1: part 1. Catalogue of the Gammaridean and Corophiidean Amphipoda (Crustacea) of the Southern Ocean, with distribution and ecological data. Bull Inst R Sci Nat Belg Biol 77:1–324

d'Udekem d'Acoz C, Havermans C (2015) Contribution to the systematics of the genus *Eurythenes* S.I. Smith in Scudder, 1882 (Crustacea: Amphipoda: Lysianassoidea: Eurytheneidae). Zootaxa 3971:1–80. doi:10.11646/zootaxa.3971.1.1

Escobar-Briones E, Nájera-Hillman E, Álvarez F (2010) Unique 16S rDNA sequences of *Eurythenes gryllus* (Crustacea: Amphipoda: Lysianassidae) from the Gulf of Mexico abyssal plain. Rev Mex Biodivers 81:177–185

Eustace RM, Ritchie H, Kilgallen NM, Piertney SB, Jamieson AJ (2016) Morphological and ontogenetic stratification of abyssal and hadal *Eurythenes gryllus sensu lato* (Amphipoda: Lysianassoidea) from the Peru–Chile Trench. Deep Sea Res Part I Oceanogr Res Pap 109:91–98. doi:10.1016/j.dsr.2015.11.005

France SC, Kocher TD (1996) Geographic and bathymetric patterns of mitochondrial 16S rRNA sequence divergence among deep-sea amphipods, *Eurythenes gryllus*. Mar Biol 126:633–643. doi:10.1007/bf00351330

Hasegawa M, Kurohiji Y, Takayanagi S, Sawadaishi S, Yao M (1986) Collection of fish and Amphipoda from abyssal sea-floor at 30° N–147° E using traps tied to 10.000 m wire of research vessel. Bull Tokai Reg Fish Res Lab 119:65–75

Havermans C (2016) Have we so far only seen the tip of the iceberg? Exploring species diversity and distribution of the giant amphipod *Eurythenes*. Biodiversity 17:12–25. doi:10.1080/14888386.2016.1172257

Havermans C, Sonet G, d'Udekem d'Acoz C, Nagy ZT, Martin P, Brix S, Riehl T, Agrawal S, Held C (2013) Genetic and morphological divergences in the cosmopolitan deep-sea amphipod *Eurythenes gryllus* reveal a diverse abyss and a bipolar species. PLoS One 8:e74218. doi:10.1371/journal.pone.0074218

Hill KL, Weaver AJ, Freeland HJ, Bychkov A (2003) Evidence of change in the sea of Okhotsk: implications for the north Pacific. Atmos Ocean 41:49–63. doi:10.3137/ao.410104

Katoh K, Standley DM (2013) MAFFT multiple sequence alignment software version 7: improvements in performance and usability. Mol Biol Evol 30:772–780. doi:10.1093/molbev/mst010

Kawabe M, Fujio S (2010) Pacific ocean circulation based on observation. J Oceanogr 66:389–403. doi:10.1007/s10872-010-0034-8

Lanfear R, Frandsen PB, Wright AM, Senfeld T, Calcott B (2017) PartitionFinder 2: new methods for selecting partitioned models of evolution for molecular and morphological phylogenetic analyses. Mol Biol Evol 34:772–773. doi:10.1093/molbev/msw260

Lilljeborg W (1865) On the *Lysianassa magellanica* H. Milne Edwards, and on the Crustacea of the suborder Amphipoda and subfamily Lysianassina found an the coast of Sweden and Norway. The Royal Acad. Press, Upsala. doi:10.5962/bhl.title.6806

Lowry JK, Stoddart HE (1995) The Amphipoda (Crustacea) of Madang lagoon: Lysianassidae, Opisidae, Uristidae, Wandinidae and Stegocephalidae. Rec Aust Mus Suppl 22:97–174. doi:10.3853/j.0812-7387.22.1995.122

Nagano A, Ichikawa H, Miura T, Ichikawa K, Konda M, Yoshikawa Y, Obama K, Murakami K (2007) Current system east of the Ryukyu Islands. J Geophys Res Oceans 112:C06009. doi:10.1029/2006JC003917

Nakano T (2012a) A new species of *Orobdella* (Hirudinida, Arhynchobdellida, Gastrostomobdellidae) and redescription of *O. kawakatsuorum* from Hokkaido, Japan with the phylogenetic position of the new species. ZooKeys 169:9–30. doi:10.3897/zookeys.169.2425

Nakano T (2012b) A new sexannulate species of *Orobdella* (Hirudinida, Arhynchobdellida, Orobdellidae) from Yakushima Island, Japan. ZooKeys 181:79–93. doi:10.3897/zookeys.181.2932

Rambaut A, Drummond AJ (2013) Tracer v1.6. Home page at: http://tree.bio.ed.ac.uk/software/tracer/. Accessed 24 May 2015

Ritchie H, Jamieson AJ, Piertney SB (2015) Phylogenetic relationships among hadal amphipods of the superfamily Lysianassoidea: implications for taxonomy and biogeography. Deep Sea Res Part I Oceanogr Res Pap 105:119–131. doi:10.1016/j.dsr.2015.08.014

Ronquist F, Teslenko M, van der Mark P, Ayres DL, Darling A, Höhna S, Larget B, Liu L, Suchard MA, Huelsenbeck JP (2012) MrBayes 3.2: efficient Bayesian phylogenetic inference and model choice across a large model space. Syst Biol 61:539–542. doi:10.1093/sysbio/sys029

Scudder SH (1882) Nomenclator Zoologicus. An alphabetical list of all generic names that have been employed by naturalists for recent and fossil animals from the earliest times to the close of the year 1879. In two parts: I. Supplemental list. II. Universal index. U.S. National Museum, Washington

Stamatakis A (2014) RAxML version 8: a tool for phylogenetic analysis and post-analysis of large phylogenies. Bioinformatics 30:1312–1313. doi:10.1093/bioinformatics/btu033

Stoddart HE, Lowry JK (2004) The deep-sea lysianassoid genus *Eurythenes* (Crustacea, Amphipoda, Eurytheneidae n. Fam.). Zoosystema 26:425–468

Talley LD (2001) Okhotsk Sea circulation. In: Steele JH, Thorpe SA (ed) Encyclopedia of ocean sciences, 1st edn. Academic Press, Oxford, pp 2007–2015. doi:10.1006/rwos.2001.0384

Tanabe AS (2008) Phylogears v2.0.2014.03.08. Home page at: http://www.fifthdimension.jp/. Accessed 24 May 2015

Thoppil PG, Metzger EJ, Hurlburt HE, Smedstad OM, Ichikawa H (2016) The current system east of the Ryukyu Islands as revealed by a global ocean reanalysis. Prog Oceanogr 141:239–258. doi:10.1016/j.pocean.2015.12.013

Thurston MH, Petrillo M, Della Croce N (2002) Population structure of the necrophagous amphipod *Eurythenes gryllus* (Amphipoda: Gammaridea) from the Atacama Trench (south-east Pacific Ocean). J Mar Biol Assoc UK 82:205–211. doi:10.1017/S0025315402005374

Tomikawa K, Nakano T, Sato A, Onodera Y, Ohtaka A (2016a) A molecular phylogeny of *Pseudocrangonyx* from Japan, including a new subterranean species (Crustacea, Amphipoda, Pseudocrangonyctidae). Zoosyst Evol 92:187–202. doi:10.3897/zse.92.10176

Tomikawa K, Tanaka H, Nakano T (2016b) A new species of the rare genus *Priscomilitaris* from the Seto Inland Sea, Japan (Crustacea, Amphipoda, Priscomilitaridae). ZooKeys 607:25–35. doi:10.3897/zookeys.607.9379

Umezu T (1982) Deep-sea pelagos. Part II. Collection by RV KAIYO-Maru for radionuclide analysis. Aquabiology (Tokyo) 4:2–9

Umezu T (1984) Deep-sea biomass in North Pacific polar frontal zone 40° N–150° E: collected by KOC-net from 150–4500 m depth in May 1981. Bull Tokai Reg Fish Res Lab 113:115–139

Zhang Z, Zhao W, Tian J, Yang Q, Qu T (2015) Spatial structure and temporal variability of the zonal flow in the Luzon Strait. J Geophys Res Oceans 120:759–776. doi:10.1002/2014JC010308

Zhao X, Zhou C, Zhao W, Tian J, Xu X (2016) Deepwater overflow observed by three bottom-anchored moorings in the Bashi Channel. Deep Sea Res Part I Oceanogr Res Pap 110:65–74. doi:10.1016/j.dsr.2016.01.007